HHS Public Access

Author manuscript

Electroanalysis. Author manuscript; available in PMC 2023 May 22.

Published in final edited form as:

Electroanalysis. 2022 December ; 34(12): 1913–1927. doi:10.1002/elan.202100580.

Separation and Detection of Tyrosine and Phenylalanine-derived Oxidative Stress Biomarkers Using Microchip Electrophoresis with Electrochemical Detection

Dhanushka B. Weerasekara[a,b], **Susan M. Lunte**[a,b,c]

[a]Ralph N. Adams Institute for Bioanalytical Chemistry, University of Kansas, Lawrence, KS, USA

[b]Department of Chemistry, University of Kansas, Lawrence, KS, USA

[c]Department of Pharmaceutical Chemistry, University of Kansas, Lawrence, KS, USA

Abstract

A method for the determination of selected aromatic amino acid biomarkers of oxidative stress using microchip electrophoresis with electrochemical detection is described. The separation of the major reaction products of phenylalanine and tyrosine with reactive nitrogen and oxygen species was accomplished using ligand exchange micellar electrokinetic chromatography with a PDMS/glass hybrid chip. Electrochemical detection was achieved using a pyrolyzed photoresist film working electrode. The system was evaluated for the analysis of the products of the Fenton reaction with tyrosine and phenylalanine, and the reaction of peroxynitrite with tyrosine.

Keywords

reactive nitrogen and oxygen species; microchip electrophoresis with electrochemical detection; hydroxyl radical; peroxynitrite; tyrosine

1. Introduction

Reactive nitrogen and oxygen species (RNOS) are a group of free radical and non-radical molecules that are generated from enzymatic and nonenzymatic processes in cells. These molecules are highly reactive and short-lived *in vivo* [1]. Under normal cellular conditions, the production of RNOS is kept at homeostasis by a defense system of antioxidants and related enzymes [2]. An increase in the production of RNOS in the cell due to the imbalance between the formation and elimination of these species *in vivo* is known as oxidative and nitrosative stress [2-3]. RNOS, such as hydroxyl radicals and peroxynitrite, can react with cell macromolecules including lipids, DNA and proteins, leading to structural and functional changes that ultimately result in cellular injury and death [4]. Oxidative and nitrosative stress has been linked to cardiovascular disease [5], cancer [6], and neurodegenerative diseases, such as Alzheimer's [7], and Parkinson's [8] disease.

slunte@ku.edu .

Supporting information for this article is available on the WWW under https://doi.org/10.1002/elan.202100580

Free and protein-bound tyrosine and phenylalanine residues are prone to undergo structural and functional modifications as a result of reactions with RNOS under oxidative/nitrosative stress conditions [9-10]. Tyrosine can exist as three different isomers, *i.e.,* para-, meta- and ortho-tyrosine (p-Tyr, m-Tyr and o-Tyr, respectively). Under physiological conditions, phenylalanine hydroxylase converts L-phenylalanine to L-p-Tyr, which is the only known isoform produced enzymatically *in vivo* [11]. However, under oxidative stress conditions, hydroxyl radicals can react with phenylalanine to produce the other two isomers, m-Tyr and o-Tyr. In addition, the reaction of hydroxyl radicals with naturally occurring L-p-Tyr can result in the formation of 3,4-dihydroxyphenylalanine (L–DOPA) [12]. Therefore, m-Tyr, o-Tyr and L–DOPA are all regarded as free radical biomarkers *in vivo* [11-13]. Peroxynitrite is produced *in vivo* through the reaction of nitric oxide and superoxide. The reaction of peroxynitrite with both free and protein bound L-p-Tyr can lead to the formation of 3-nitrotyrosine (NT) and 3,3'-dityrosine (di-Tyr). The protonated form of peroxynitrite, peroxynitrous acid (ONOOH), can also generate hydroxyl radicals that can react with phenylalanine to produce m-Tyr and o-Tyr [14-15] (Figure 1). Therefore, all six of these modified phenylalanine and tyrosine products can be used as biomarkers of oxidative stress in the brain and other tissues.

A wide variety of separation-based methods have been used to investigate the oxidative products of tyrosine and phenylalanine [16-19]. Separation and detection of the tyrosine isomers has been accomplished by liquid chromatography (LC) using UV [20-22], mass spectrometry [23] and fluorescence [24] detection. The simultaneous determination of nitrotyrosine and tyrosine in human urine and animal tissue has been reported using LC-UV [25] and LC–MS/MS [26], respectively. LC with fluorescence detection has also been employed to separate and quantify underivatized L–DOPA and tyrosine in reaction mixtures containing either purified or crude catalase enzyme preparations [27]. Since the majority of the products of RNOS with tyrosine and phenylalanine are electroactive at modest potentials, liquid chromatography with electrochemical detection has also been used for the direct detection of tyrosine, 3-nitrotyrosine and 3,3'-dityrosine from protein digests of human brain specimens [28]. In one study, LC with dual electrode detection was used for the determination of the tyrosine isomers, 3-nitrotyrosine and L–DOPA in rat plasma samples [29].

Capillary electrophoresis (CE) is a useful method for the highly efficient separation of charged analytes and has been used extensively for amino acid separations [30]. CE-MS has been used for the determination of L–DOPA, tyrosine and NT in biological samples [31-33]. CE with UV detection has been previously reported for the determination of 3-nitrotyrosine in urine [34]. It has also been used to separate and detect p-Tyr and NT standards using micellar electrokinetic chromatography [35]. In that application, sodium dodecyl sulfate (SDS) was employed to enhance the resolution of tyrosine and NT. CE has also been explored for chiral separations of tyrosine and other amino acids using ligand exchange chromatography [36]. In particular, the use of a L-4-hydroxyproline – Cu(II) complex as a chiral selector for the separation of amino acid enantiomers, including tyrosine, has been investigated [37-38]. Most relevant to our work is the report by Chen *et al.* where they used a combination of ligand-exchange and micellar electrokinetic chromatography (LE-MEKC). A background electrolyte containing the copper(II)-4-hydroxyproline complex along with

SDS was employed to facilitate the separation of p-, m- and o-tyrosine and their respective enantiomers by CE-UV [39].

Microchip electrophoresis (ME) is a miniaturized version of CE and has many advantages over more conventional separation-based analytical systems, such as liquid chromatography, for the separation of these biomarkers as well as enantiomeric separations [40-42]. Compared to LC, separation times of ME are faster (2–3 minutes) and require much smaller sample volumes. With ME, it is also possible to use background electrolytes containing additives that would be too expensive or not compatible with the stationary phases used in LC. The detection instrumentation required for LC or CE systems is generally more expensive and complex than that employed for ME. There are several modes of detection for ME, with fluorescence detection being the most popular. However, electrochemical detection (EC) is an ideal detection method for the determination of aromatic amino acid biomarkers of oxidative stress because, as previously mentioned, most of these compounds are electrochemically active. This mode of detection also has several additional advantages for ME. Electrodes can be integrated directly into the chip using conventional micro-fabrication methods, and different electrode materials are available to enhance selectivity. The associated electronics are also inexpensive and can be easily miniaturized to generate portable analysis systems [41, 42].

In this paper, a comprehensive ME-EC method for the separation and detection of six of the major products of the reaction of phenylalanine and tyrosine with hydroxyl radicals or peroxynitrite is reported. A LE-MEKC method was developed that was compatible with ME-EC for the determination of all three isomeric tyrosines, 3-nitrotyrosine, L–DOPA and 3,3’-dityrosine. The method was demonstrated by analyzing the products of reactions of phenylalanine and tyrosine with hydroxyl radicals generated by the Fenton reaction and in-house synthesized peroxynitrite.

2. Experimental

2.1 Reagents and Solutions

L-p-tyrosine and 3,4-dihydroxy-L-phenylalanine (L–DOPA) and nitrilotriacetic acid were purchased from Sigma-Aldrich (St. Louis, MO, USA). 3-L-nitrotyrosine, DL-m-tyrosine, DL-o-tyrosine, DL-phenylalanine, 4-hydroxy-L-proline, copper(II) sulfate, SDS, sodium acetate, acetic acid, ammonium hydroxide, hydrogen peroxide, isopropyl alcohol and iron(II) sulfate were obtained from Fisher Scientific (Pittsburgh, PA, USA). 3,3’-Dityrosine was synthesized by the Synthetic Chemical Biology Core Laboratory at the University of Kansas (Lawrence, KS, USA). The following materials were purchased and used for microchip and electrode fabrication: quartz glass plates (4 in × 2.5 in × 0.085 in, Glass Fab, Rochester, NY, USA); AZ 1518 positive photoresist and AZ 300 MIF developer (AZ Electronic Materials, Somerville, NJ, USA); SU-8 10 negative photoresist and SU-8 10 developer (Micro-Chem, Newton, MA, USA); polydimethylsiloxane (Sylgard™ 184) silicon elastomer base and curing agent (Dow Corning Corp., Midland, MI, USA); copper wire (22-gauge, ACE Hardware, Lawrence, KS, USA); epoxy glue (J–B Weld, Sulphur Springs, TX, USA), and colloidal silver liquid (Ted Pella, Inc., Redding, CA, USA). All the solutions were prepared in 18.2 MΩ.cm Milli-Q water (Millipore, Kansas City, MO, USA).

2.2 Fabrication of PDMS Microchip

The fabrication of PDMS microchips has been described previously [43]. Briefly, SU–8 10 negative photoresist was spin coated onto a 4 in silicon wafer using a Cee 100 spin coater (Brewer Science, Rolla, MO) at 1650 rpm for 30 s to obtain a 15 μm thick layer. The film was baked for 3 min at 95 °C. Channel features were created using Autodesk AutoCad software (San Rafael, CA, USA) and printed on a transparency film to use as a negative photomask. A simple "t" design containing a 5 cm long separation channel and 0.75 cm long top and side arms (unless mentioned otherwise) was used. All channels were 40 μm wide. The negative photomask was placed on top of the coated silicon wafer and exposed to UV light (15 mW. cm^{-2}) for 10 s using a UV flood source (AMB Inc., Scotts Valley, CA, USA). Using a programmable hot plate (Thermo Scientific, Waltham, MA, USA), the silicon wafer was baked for 3 min at 95 °C. The silicon master was then developed (using SU-8 10 developer) and rinsed with isopropyl alcohol. It was dried with N_2 gas and baked in an oven at 200 °C for 2 hours. A total of 12 g of PDMS elastomer base/curing agent was mixed at a ratio of 10:1 (base:curing agent) and poured onto the silicon master to create the PDMS microchip. The PDMS was then allowed to cure at 70 °C overnight in an oven, cooled to room temperature, and removed from the silicon master for experimental use. The holes for the sample, buffer, buffer waste and sample waste reservoirs were produced using a 4 mm biopsy punch (Harris uni-Core, Ted Pella, Inc., Redding, CA, USA).

2.3 Fabrication of Pyrolyzed Photoresist Film (PPF) Carbon Electrode

The fabrication of the PPF carbon electrode was accomplished as previously described by our group [44]. Briefly, AZ-1518 positive photoresist was deposited onto a clean quartz glass plate (2.5 × 4 inch) using a Cee 100 spin coater at 100 rpm for 10 s. The spin coater was ramped to 2000 rpm and held for 20 s. The coated plate was then baked for 3 min at 100 °C on a hot plate. The coated glass plate was covered with a positive photomask that contained the electrode features and exposed to UV light (15 $mW.cm^{-2}$) for 13 s. The plate was developed using AZ 300 MIF developer and rinsed with NANOpure water, followed by drying with N_2 gas. The plate with the photoresist feature was post-baked at 100 °C for 10 min and then placed inside a Linden-Blue 3 Zone tube furnace (Cole-Palmer, Vernon Hill, IL, USA) under 5 psi N_2 gas flow. The temperature of the furnace was increased from room temperature to 925 °C at a rate of 5.5 °C/min and held at 925 °C for 1 hour. The final dimensions of the electrodes on the glass plates were 35 μm in width and 420–480 nm in height, which was determined by a Profilm3D optical profilometer (Filmetrics, San Diego, CA, USA).

2.4 Microchip Electrophoresis Separation Procedure

The PDMS/glass hybrid chip was produced by carefully positioning the PDMS layer on the glass with the PPF working electrode with reversible bonding (Figure 2a). The glass containing the PPF electrode was washed with isopropyl alcohol and Milli-Q water and air dried prior to bonding with PDMS. The electrode and separation channel were conformally aligned to a pseudo-end channel configuration (Figure 2b).

The channels of the microchip were flushed with isopropyl alcohol, Milli-Q water and then with background electrolyte (BGE) for approximately 5 minutes each prior to

electrophoresis. The BGE was freshly prepared before each set of experiments and was filtered using a 0.22 μm filter prior to use. For the separation, an UltraVolt high voltage power supply (Ronkonkoma, NY, USA) was used, which was controlled by a LabView program (National Instruments, Austin, TX, USA) written in-house. For these studies, sample introduction was accomplished utilizing an electrokinetic gated injection method. Here, a "gate" was created at the junction of the simple "t" device by applying + 1900 V at the sample reservoir (+ 2700 V for the 7 cm chip) and +1600 V at the buffer reservoir (+ 2400 V for the 7 cm chip) while keeping the other two reservoirs (sample waste and buffer waste) grounded. Sample was injected into the separation channel by floating the voltage at the buffer reservoir for 1.0s (0.7 s for 7 cm chip) and then the voltages were restored for separation. Freshly prepared BGEs (different compositions of L-4-hydroxyproline, $CuSO_4$ and SDS) and standards prepared in Milli-Q water (25 μM each, unless otherwise noted) were used for these experiments. Samples were injected into the device after a stable baseline was observed when the buffer and sample reservoir potentials were applied. In between each sample, an injection of BGE was made to flush the system prior to the injection of the next sample. During ME-EC experiments, deposition of copper onto the Pt leads that were used to connect the microchip to the electrophoresis power supply was sometimes seen (but only on the Pt leads in the waste reservoirs). When this was observed, the electrodes were cleaned using 10% HNO_3 and then Milli-Q water prior to the next run.

2.5 Electrochemical Detection

Electrochemical detection in these studies was accomplished using an electrically isolated potentiostat (Pinnacle Technology, Inc., Lawrence, KS, USA). A two-electrode (carbon PPF working electrode and Ag/AgCl reference electrode) system was utilized where a detection potential of + 1.1V (vs. Ag/AgCl reference electrode) was applied to the working electrode. The data sampling rate was set to 10 Hz and data acquisition was carried out wirelessly through Sirenia software (Pinnacle Acquisition Laboratory).

2.6 Cyclic Voltammetry

Cyclic voltammetry (CV) measurements were performed using an 812 C potentiostat (CH Instruments, Austin, TX, USA). The electrochemical cell consisted of a 3 mm diameter glassy carbon working electrode (CH Instruments), a Ag/AgCl reference electrode (Bioanalytical Systems, West Lafayette, IN, USA) and a platinum wire counter electrode. The surface of the glassy carbon electrode was renewed by mechanically polishing the surface with alumina slurry (Bioanalytical Systems) and rinsing thoroughly with Milli-Q water. Three supporting electrolytes (SE) were tested; SE1 = 0.1 M acetate at pH 4.0; SE2 = 25 mM 4-hydroxyproline and 12.5 mM $CuSO_4$ at pH 4.0; SE3 = 25 mM 4-hydroxyproline and 12.5mM $CuSO_4$ at pH 4.0 with 8 mM SDS. After adding 2.7mL of supporting electrolyte to the electrochemical cell, 0.3 mL of 2 mM p-tyrosine dissolved in Milli-Q water (final concentration = 200 μM) was added. Cyclic voltammograms were recorded at a scan rate of 100 mV/s using a 1 mV sampling rate and potential range from + 500 to +1200 mV vs. Ag/AgCl.

A separate set of CV measurements was performed for p-Tyr and NT to determine the optimal oxidation potential for their detection with ME-EC. In this case, both analytes (final

concentration = 200 μM) were dissolved in a SE containing 25 mM 4-hydroxyproline, 12.5mM $CuSO_4$ and 15 mM acetate buffer at pH 4.0 with 16.5 mM SDS. Cyclic voltammograms were recorded at a potential scan rate of 100 mV/s using a 1 mV sampling rate and potential range from + 0 to +1200 mV vs. Ag/AgCl.

2.7 Capillary Electrophoresis Separations

An Agilent 7100 capillary electrophoresis system (Agilent Technologies, Santa Clara, CA, USA) with UV detection was utilized for CE experiments. The separation was carried out using a fused silica capillary (50 μm I.D. ×356 μm O.D.) (Polymicro Molex, Lisle, IL, USA) with a total length of 56 cm and an effective length of 47.5 cm. The capillary was conditioned with subsequent flushes of 0.1 M NaOH, Milli-Q water, and the BGE for 10 minutes, prior to electrophoresis. Samples were injected using electrokinetic injection (5 s at 10 kV) and the separation was performed by applying a separation voltage of 14 kV. UV detection was performed at 208 nm.

2.8 Fenton Reaction

The Fenton reaction generates hydroxyl radicals that can then react with aromatic amino acids to produce the compounds analyzed by the ME-EC method developed here. The Fenton reaction was initiated by adding H_2O_2 (final concentration = 1 mM) to a final volume of 5 mL solution containing 1 mM $FeSO_4$, 2 mM nitrilotriacetic acid and either 5 mM DL-phenylalanine or 1 mM L-p-tyrosine in 10 mM acetate buffer at pH 5.5. The reaction mixture was incubated at room temperature for 1 hour before analysis.

2.9 Reaction of Peroxynitrite with p-Tyrosine

The synthesis of peroxynitrite was adapted from the protocol by Schilly [45]. All solutions used were freshly prepared and chilled on ice prior to use. To perform the reaction, 150 μL of a solution of 0.7 M HCl in 0.6 M H_2O_2 was added to a tube containing 200 μL of 0.6 M $NaNO_2$ and mixed. Then, 200 μL of 2 mM L-p-Tyr was added within 1–2 s of the addition of acidified H_2O_2 to $NaNO_2$. The reaction mixture was kept on ice prior to analysis, then diluted 8-fold with the background electrolyte and injected into the ME-EC system.

3. Results and Discussion

3.1 Separation Optimization of RNOS Products with Tyrosine and Phenylalanine

Initial ME-EC experiments were conducted using a PDMS/glass hybrid chip with a 5 cm separation channel. The microchip design and detection strategy are illustrated in Figure 2a. Here, several different BGEs that were previously employed by our group for the separation of catecholamine neurotransmitters were evaluated for the separation of NT, L–DOPA, and p-, m-, and o-tyrosine [43, 44]. These BGEs consisted of different combinations of phosphate and borate buffers containing SDS concentrations between 2–10 mM. Additives, such as β-cyclodextrins (1–4 mM), dimethyl sulfoxide (DMSO) and ethanol (5-10%), were also evaluated. All the BGEs tested were able to separate NT and L–DOPA from the tyrosine isomers. However, the three tyrosine isomers could not be resolved.

Chen *et al.* previously reported the separation and detection of the three tyrosine isomers by CE-UV using a L-4-hydroxyproline-copper(II) complex [39]. The proposed mechanism for the separation is shown in Figure 3. First, 4-hydroxyproline reacts with copper(II) in the ratio of 2:1 to form a complex. Upon addition of the aromatic amino acid of interest, a ternary complex is produced via a ligand exchange mechanism, where one molecule of L-4-hydroxyproline is replaced by the amino acid. The difference in formation constants for the amino acid-Cu(II)-hydroxyproline complexes results in a difference in their electrophoretic mobilities. In the work of Chen *et al.,* SDS was also introduced into the BGE to form a micellar system. The partitioning of the amino acid-Cu(II)-hydroxyproline complexes with micelles further differentiates the overall mobility of each amino acid type, thus improving the separation. This approach was successfully demonstrated by Chen *et al.* for the separation of all the tyrosine isomers and enantiomers using CE-UV [39].

Since CE and ME are based on the same separation principles, the separation of the tyrosine isomers and other tyrosine derivatives using the above mentioned BGE was tested first on a commercial CE-UV instrument before applying the LE-MEKC method to microchip electrophoresis. A BGE consisting of 50 mM 4-hydroxyproline and 25 mM $CuSO_4$ at pH 4.5 with 10 mM SDS provided a good separation of all the analytes tested (NT, L–DOPA, p-, m-, and o-tyrosine). With this BGE, it was possible to baseline resolve all the analytes of interest, including the D and L forms of m- and o-tyrosine (Figure 4). However, the CE-UV system suffered from high inconsistent background absorbance and the separation took 18 minutes.

3.1.1 Effects on BGE for the Oxidation Potential of Tyrosine—The next step was to evaluate the BGE for ME-EC analysis of these compounds. First, the effect of the LE-MEKC buffer on the electrochemical behavior of tyrosine was investigated using cyclic voltammetry. As expected, the oxidation of p-tyrosine proceeded irreversibly in all three SEs (Figure 5a). The oxidation potential of p-tyrosine in acetate buffer at pH 4.0 was shifted slightly higher when the SE was changed to Cu(II)-4-hydroxyproline complex at pH 4.0 (from 876 to 902 mV vs Ag/AgCl) and the peak current was reduced (−6.73 to −6.11 μA). However, the SE that contained the Cu(II)-4-hydroxyproline complex and SDS provided a relatively similar oxidation potential and peak current compared to those observed for p-tyrosine in acetate buffer. These results indicated that the electrochemical behavior of p-Tyr does not change drastically due to the addition of a solution containing the Cu(II)-4-hydroxyproline complex at pH 4.0 with SDS. Therefore, the Cu(II)-4-hydroxyproline complex at pH 4.0 with SDS was used as the BGE for ME-EC detection of tyrosine and its isomers.

3.1.2 Microchip Electrophoresis with Electrochemical Detection (ME-EC)—Once the separation was optimized using CE-UV and the effect of LE-MEKC BGE on the electrochemical response was determined, the method was transferred to ME-EC using a PDMS/glass hybrid chip with a 5 cm separation channel and a PPF electrode in a pseudo end-channel configuration. First, the effect of the relative concentrations of 4-hydroxyproline, copper (II) and SDS on resolution of the analytes of interest was investigated at pH 4.5. BGE concentrations of 4-hydroxyproline ranging from 20 mM to

50 mM were investigated while maintaining the ratio of 4-hydroxyproline to copper(II) at 2:1. The resolution of the three tyrosine isomers improved with increasing concentrations of L-4-hydroxyproline and $CuSO_4$. However, at concentrations greater than 25 mM, the separation current increased dramatically resulting in a high and inconsistent background current. Therefore, 25 mM L-4-hydroxyproline and 12.5 mM $CuSO_4$ were chosen as the optimum additive concentrations. To complete the LE-MEKC mechanism, the effect of SDS concentrations starting from 8 mM (CMC) and above on the separation was investigated. At 8 mM SDS, the resolution of the three tyrosine isomers, NT and L–DOPA started to improve. However, at concentrations above 10 mM SDS, there was no additional improvement in resolution, and higher SDS concentrations introduced high separation currents that damaged the microchip device. Based on these studies, a BGE consisting of 25 mM L-4-hydroxyproline and 12.5 mM $CuSO_4$ at pH 4.5 with 10 mM SDS provided the best separation for all the analytes tested (Figure 6).

3.1.3 Effect of Channel Length on Tyrosine Isomer Resolution—In an attempt to further improve the resolution of the tyrosine isomers, the effect of a longer separation channel was investigated. A PDMS/glass hybrid chip with a 7 cm separation channel was used for these studies. The separation voltages of the sample reservoir and buffer reservoir were kept at + 2700 V and + 2400 V, respectively, for gated injection and to maintain a similar field strength (232 V/cm) inside the separation channel as that was used for the 5 cm channel (222 V/cm).

A BGE consisting of 25 mM 4-hydroxyproline and 12.5 mM $CuSO_4$ at pH 4.0 containing 8 mM SDS was initially tested with the microchip device containing a 7 cm separation channel. Unfortunately, this did not result in an improved separation of the three tyrosine isomers compared to that achieved with the 5 cm channel. The effect of varying concentrations of SDS on the separation of the three tyrosine isomers was then investigated with the 7 cm channel microchip. The objective was to see whether better resolution of the peaks was achieved at SDS concentrations above the CMC (8 mM). For these experiments, the rest of the BGE constituents were kept the same (25 mM 4-hydroxyproline and 12.5 mM $CuSO_4$ at pH 4.0). It was found that the separation of the three tyrosine isomers started to improve when the SDS concentration was increased to 12 mM. Even though the resolution was further improved, at SDS concentrations of 20 mM or above, the separation currents were 10– 15 μA higher than normal (20–25 μA). Therefore, a SDS concentration in the range of 16–16.5 mM was considered the best compromise between resolution and separation current generation and was used for all future experiments.

3.14 Addition of Ammonium Acetate to the BGE—One issue that was observed with the BGE described above was high run-to-run variablilty in migration times for the analytes of interest. The %RSD values for migration times were between 4 and 5 % for all analytes for multiple injections (n = 3) on the same 7 cm microchip. It was hypothesized that this variability could be due to a gradual change in BGE pH during the electrophoresis process because the system was not well buffered. To improve the buffer capacity of the system, ammonium acetate was introduced into the BGE. It was found that the addition of

10 mM ammonium acetate to the BGE significantly improved migration reproducibilty with RSD values of approximately 1 % (Table 1).

A BGE consisting of 25 mM 4-hydroxyproline and 12.5 mM Cu(II) containing 16.5 mM SDS and 10 mM ammonium acetate at pH 4.0 was tested for the separation of all of six analytes of interest (L–DOPA, p-Tyr, m-Tyr, o-Tyr, NT and di-Tyr). The resulting separation is shown in Figure S1. Most of the analytes are baseline resolved. The ammonium acetate concentration was then increased to 15 mM and baseline resolution of all of the analytes was accomplished. Therefore, this BGE was used for all further experiments. It should also be noted that the analyte stock solutions used in these experiments contained the D and L enantiomers of o-Tyr and m-Tyr, since these compounds are only commercially available as racemic mixtures. As can be seen in the electropherograms in Figure 7 and S1, the peak for o-Tyr is split into two, indicating the separation of the two enantiomers of o-Tyr along with the other analytes of interest. In Figure S1, the m-Tyr enantiomers were also separated.

3.2 Analysis of Fenton Reaction Products of Phenylalanine and Tyrosine by ME-EC

The optimized ME-EC method was then evaluated for the analysis of the reaction products of DL- phenylalanine with the hydroxyl radical as generated by the Fenton reaction. The Fenton reaction is a well described system for the production of hydroxyl radicals (•OH) [46]. In this reaction, •OH is generated by the reduction of H_2O_2 in the presence of Fe(II). It has also been shown that some chelating ligands, such as nitrilotriacetic acid (NTA), can accelerate the catalytic activity of Fe(II) when these chelators form complexes with Fe(II) [21, 47-48]. In a separate study, Maskos *et al.* reported that the reaction of Phe or Tyr with •OH generates the maximum yield of hydroxylated products at pH 5.5 [49]. Therefore, in our studies, Fe(II)-nitrilotriacetic acid was reacted with H_2O_2 in the presence of 5 mM DL-phenylalanine in 10 mM acetate buffer at pH 5.5. The reaction conditions were adapted from a previously published procedure on the Fenton reaction with phenylalanine [21].

In these experiments, the reaction of phenylalanine with Fenton reaction was performed at room temperature and allowed to progress for approximately 1 hour. The mixture was then diluted 2-fold with 10 mM acetate buffer at pH 4.0 and injected into the ME-EC system containing BGE (25 mM 4-hydroxyproline, 12.5 mM $CuSO_4$, 15 mM acetate buffer at pH 4.0 and 16.5 mM SDS). As can be seen in Figure 8a, all three tyrosine isomers were observed in the electropherogram. Here, the stock solution of phenylalanine contained both D and L forms, and as a result, all the enantiomers of p-, m- and o-Tyr were also produced as indicated in Figure 8a by the spilt peaks for p-, m- and o-Tyr peaks in the electropherogram.

Relative standard deviations (%RSD) of the peak heights of p-, m- and o-Tyr peaks for the Fenton reaction were within the range of 4–5 % (n = 3) while for a mixture of standards (50 μM each), the %RSD for the peak heights of p-, m- and o-Tyr were within the range of 3–6% (n = 3). This result indicates that the injection of Fenton reaction solution into the chip does not have an apparent effect on the electrochemical response of the PPF working electrode compared to the BGE. Literature suggests two additional products, L–DOPA and 2,3-dihydroxyphenylalanine, are generated by the further hydroxylation of phenylalanine by hydroxyl radical during the Fenton reaction [48]. However, neither product was detected in these ME-EC experiments.

ME-EC was also used to investigate the products of L-p-tyrosine in the Fenton reaction. Again, the reaction mixture was diluted 2-fold with 10 mM acetate buffer at pH 4.0 and injected into the microchip containing BGE (25 mM 4-hydroxyproline, 12.5 mM $CuSO_4$, 15 mM acetate buffer at pH 4.0 and 16.5 mM SDS). In this case, the production of L–DOPA was observed as seen in Figure 8b. Similarly to the results obtained with the Fenton reaction and Phe, there was no significant change in the %RSD for peak heights for the products of Fenton reaction with L-p-tyrosine compared to that of the standards. However, in the electropherogram for the Fenton reaction solution, an unknown peak was observed (Peak 3 in Figure 8b). The magnitude of this peak increased substantially with each injection from the sample reservoir, indicating that Fenton reaction could still be in progress during the electrophoretic analysis.

3.3 ME-EC Separation and Detection of Reaction Products of Peroxynitrite and p-Tyrosine

Peroxynitrite is generated *in vivo* by the reaction of superoxide and nitric oxide. Its protonated form, peroxynitrous acid, can by synthesized using acidified H_2O_2 and $NaNO_2$ [50]. Peroxynitrous acid (pKa ~6.8) has a short half-life of less than one second under acidic conditions and undergoes homolysis to produce $NO_2^{\bullet}$ and $^{\bullet}OH$ radicals that can react with aromatic amino acids [50-51]. To ensure that L-p-Tyr has enough time to react with peroxynitrous acid, L-p-Tyr was added within 1–2 s following the addition of acidified H_2O_2 to $NaNO_2$. The instantaneous formation and disappearance of a yellow color suggested the formation and fast degradation of the peroxynitrous acid. Figure 9 shows the electropherograms for the reaction mixture of peroxynitrite and a standard mixture containing L-p-Tyr and NT. Only one prominent peak was observed in the reaction mixture, and it was identified as NT based on its migration time and spiking the sample with NT standard. Since L-p-Tyr was the limiting reagent in this reaction, its complete conversion to NT was not unexpected. To further confirm the identity of NT, ME-EC analysis of the sample and standards was performed at two different oxidation potentials (+ 1.1V and + 0.9 V vs. Ag/AgCl). First, analysis of the mixture containing authentic p-Tyr and NT at the two different working electrode potentials (+1.1 V and + 0.9 V vs Ag/AgCl) was performed. The results were then compared to the electropherograms obtained for the reaction mixture at the same detection potentials. Although the NT peak was detected at +1.1 V in both electropherograms, it was not present in either the sample or the standard mixture at + 0.9 V vs. Ag/AgCl (Figure 9). As can be seen in the cyclic voltammograms in Figure 5b, the oxidation of NT in this BGE occurs at a much higher oxidation potential (+1.0 V vs Ag/AgCl) than p-Tyr (+ 0.85 V vs. Ag/AgCl). Therefore, this difference in electrochemical behavior can be used to further verify the reaction product as NT.

It has been reported that Tyr can be oxidized to $Tyr^{\bullet}$ by either $NO_2^{\bullet}$ or $^{\bullet}OH$ to generate L–DOPA or di-Tyr, along with NT [52]. However, these products were not observed under the experimental conditions used in these analyses. It should be noted that in these studies, the reaction mixture of peroxynitrite with p-Tyr was diluted 8-fold with the BGE before it was injected into the microchip. Less dilute samples generated high separation currents that damaged the microchip. Therefore, there is the possibility that products such as L–DOPA and di-Tyr were not observed in the electropherogram due to the dilution of the sample.

4. Conclusion and Future Directions

In this work, the optimization of a ME-EC system for the separation and detection of modified phenylalanine and tyrosine biomarkers of oxidative stress is described. Under optimal conditions, six compounds including 3-nitrotyrosine, L–DOPA, 3,3'-dityrosine and p-, m- and o-tyrosine were separated and detected with an analysis time of less than two minutes. The method was applied to the analysis of products generated by model systems used for the production of •OH and peroxynitrite. Using MEEC, the reaction products of tyrosine with hydroxyl radicals or peroxynitrite as well as phenylalanine with hydroxyl radicals were analyzed and tentatively identified based on migration times, spiking with standards and electrochemical behavior. In future studies, this method will be applied to profile oxidative and nitrosative modifications of these residues that occur in small tyrosine- and phenylalanine-containing peptides.

Supplementary Material

Refer to Web version on PubMed Central for supplementary material.

Acknowledgements

Dr. Lunte would like to gratefully acknowledge Professor Ted Kuwana for all his mentoring and guidance throughout her career since her arrival at the University of Kansas in 1987. The authors would also like to thank Dr. Manjula Wijesinghe for helpful discussions and the invaluable assistance of Dr. Shamal Gunawardhana and Indika Warnakula with electrode fabrication. In addition, authors would like to thank Riley Stegmaier for the preparation of peroxynitrite-tyrosine reaction. The device fabrication was performed at the Ralph N. Adams Institute COBRE Core Nanofabrication Facility (NIH P20GM103638). This research was supported by a research grant from University of Kansas School of Medicine Landon Center on Aging (NIH P30 AG035982). Part of this work was presented (poster) at the International Conference on Miniaturized Systems for Chemistry and Life Sciences (μTAS), Basel, Switzerland, 2019.

Data Availability Statement

The data that support the findings of this study are available from the corresponding author upon reasonable request.

References

[1]. Ozcan A, Ogun M in Basic principles and clinical significance of oxidative stress,1st *ed., Vol.*3 (Ed.:Gowder SJT), IntechOPen, Croatia, 2015, 37–58.

[2]. Ye Z-W, Zhang J, Townsend DM, Tew KD, Biochim. Biophys. Acta Gen. Subj 2015, 1850, 1607–1621.

[3]. Lichtenberg D, Pinchuk I, Biochem. Biophys. Res. Commun 2015, 461, 441–444. [PubMed: 25911322]

[4]. Pisoschi AM, Pop A, Iordache F, Stanca L, Predoi G, Serban AI, Eur. J. Med. Chem 2020, 112891. [PubMed: 33032084]

[5]. Senoner T, Dichtl W, Nutrients 2019, 11, 2090. [PubMed: 31487802]

[6]. Hayes JD, Dinkova-Kostova AT, Tew KD, Cancer Cell 2020.

[7]. Huang WJ, Zhang X, Chen WW, Biomed. Rep 2016, 4, 519–522. [PubMed: 27123241]

[8]. Hauser DN, Hastings TG, Neurobiol. Dis 2013, 51, 35–42. [PubMed: 23064436]

[9]. Feeney MB, Schoneich C, Antioxid. Redox Signaling 2012, 17, 1571–1579.

[10]. Ipson BR, Fisher AL, Ageing Res. Rev 2016, 27, 93–107. [PubMed: 27039887]

[11]. Molnár GA, Kun S, Sélley E, Kertész M, Szélig L, Csontos C, Böddi K, Bogár L, Miseta A, Wittmann I, Curr. Med. Chem 2016, 23, 667–685. [PubMed: 26785996]

[12]. Molnár GA, Nemes V, Biró Z, Ludány A, Wagner Z, Wittmann I, Free Radical Res. 2005, 39, 1359–1366. [PubMed: 16298866]

[13]. Molnár GA, Mikolás EZ, Szijártó IA, Kun S, Sélley E, Wittmann I, World J. Diabetes 2015, 6, 500–507. [PubMed: 25897359]

[14]. van der Vliet A, O'Neill CA, Halliwell B, Cross CE, Kaur H, FEBS Lett. 1994, 339, 89–92. [PubMed: 8313984]

[15]. Pfeiffer S, Schmidt K, Mayer B, J. Biol. Chem 2000, 275, 6346–6352. [PubMed: 10692434]

[16]. Houée-Lévin C, Bobrowski K, Horakova L, Karademir B, Schöneich C, Davies MJ, Spickett CM, Free Radical Res. 2015, 49, 347–373. [PubMed: 25812585]

[17]. Bandookwala M, Thakkar D, Sengupta P, Crit. Rev. Anal. Chem 2020, 50, 265–289. [PubMed: 31177807]

[18]. Teixeira D, Fernandes R, Prudêncio C, Vieira M, Biochimie 2016, 125, 1–11. [PubMed: 26921794]

[19]. DiMarco T, Giulivi C, Mass Spectrom. Rev 2007, 26, 108–120. [PubMed: 17019703]

[20]. Biondi R, Brancorsini S, Poli G, Egidi MG, Capodicasa E, Bottiglieri L, Gerli S, Brillo E, Renzo GCD, Cretoiu D, Micu R, Suciu N, Talanta 2018, 181, 172–181. [PubMed: 29426497]

[21]. Biondi R, Xia Y, Rossi R, Paolocci N, Ambrosio G, Zweier JL, Anal. Biochem 2001, 290, 138–145. [PubMed: 11180947]

[22]. Al-Sadoon I, Wittmann I, Kun S, Ahmann M, Konyi A, Verzár Z, J. Clin. Lab. Anal 2021, 35, e23613. [PubMed: 33043503]

[23]. Ruggiero RA, Bruzzo J, Chiarella P, di Gianni P, Isturiz MA, Linskens S, Speziale N, Meiss RP, Bustuoabad OD, Pasqualini CD, Cancer Res. 2011, 71, 7113–7124. [PubMed: 22084446]

[24]. Ishimitsu S, Fujimoto S, Ohara A, J. Chromatogr 1986, 378, 222–225. [PubMed: 3733974]

[25]. Du M, Wu W, Ercal N, Ma Y, J. Chromatogr. B 2004, 803, 321–329.

[26]. Torres-Cuevas I, Kuligowski J, Cárcel M, Cháfer-Pericás C, Asensi M, Solberg R, Cubells E, Nuñez A, Saugstad OD, Vento M, Escobar J, Anal. Chim. Acta 2016, 913, 104–110. [PubMed: 26944994]

[27]. Olšovská J, Novotná J, Flieger M, Spížek J, Biomed. Chromatogr 2007, 21, 1252–1258. [PubMed: 17604359]

[28]. Hensley K, Maidt ML, Yu Z, Sang H, Markesbery WR, Floyd RA, J. Neurosci 1998, 18, 8126–8132. [PubMed: 9763459]

[29]. Kumarathasan P, Vincent R, J. Chromatogr. A 2003, 987, 349–358. [PubMed: 12617061]

[30]. Poinsot V, Bayle C, Couderc F, Electrophoresis 2003, 24, 4047–4062. [PubMed: 14661233]

[31]. Yuan B, Wu H, Sanders T, McCullum C, Zheng Y, Tchounwou PB, Liu Y-M, Anal. Biochem 2011, 416, 191–195. [PubMed: 21683678]

[32]. Hao L, Zhong X, Greer T, Ye H, Li L, Analyst 2015, 140, 467–475. [PubMed: 25429371]

[33]. Hirayama A, Tomita M, Soga T, Analyst 2012, 137, 5026–5033. [PubMed: 23000847]

[34]. Ren H, Liu X, Jiang S, J. Pharm. Biomed. Anal 2013, 78–79, 100–104.

[35]. Li H-L, Xu H-B, Gao Z-H, J. Anal. Chem 2007, 35, 1087–1091.

[36]. Chen Z, Uchiyama K, Hobo T, Enantiomer 2001, 6, 19–25. [PubMed: 11434537]

[37]. Schmid MG, Rinaldi R, Dreveny D, Gübitz G, J. Chromatogr. A 1999, 846, 157–163.

[38]. Schmid MG, Grobuschek N, Lecnik O, Gübitz G, J. Biochem. Biophys. Methods 2001, 48, 143–154. [PubMed: 11356484]

[39]. Chen Z, Lin J-M, Uchiyama K, Hobo T, J. Chromatogr. A 1998, 813, 369–378.

[40]. Belder D, in Chiral Analysis, Elsevier, 2006, pp. 277–295.

[41]. Costa BMDC, Griveau S, d'Orlye F, Bedioui F, da Silva JAF, Varenne A, Electrochim. Acta 2021, 391, 138928.

[42]. Schilly KM, Gunawardhana SM, Wijesinghe MB, Lunte SM, Anal. Bioanal. Chem 2020, 412, 6101–6119. [PubMed: 32347360]

[43]. Saylor RA, Reid EA, Lunte SM, Electrophoresis 2015, 36, 1912–1919. [PubMed: 25958983]

[44]. Gunawardhana SM, Bulgakova GA, Barybin AM, Thomas SR, Lunte SM, Analyst 2020, 145, 1768–1776. [PubMed: 31915763]

[45]. Schilly KM, Ph.D Thesis, University of Kansas, Lawrence, KS, 2021.

[46]. Winterbourn CC, Toxicol. Lett 1995, 82–83, 969–974.

[47]. Miller CJ, Rose AL, Waite TD, Frontiers in Marine Science 2016, 3, 134.

[48]. Zhang Y, Zhou M, J. Hazard. Mater 2019, 362, 436–450. [PubMed: 30261437]

[49]. Maskos Z, Rush JD, Koppenol WH, Arch. Biochem. Biophys 1992, 296, 521–529. [PubMed: 1321588]

[50]. Robinson KM, Beckman JS, in Methods in Enzymology, *Vol.* 396, Academic Press, 2005, pp. 207–214. [PubMed: 16291234]

[51]. Carballal S, Bartesaghi S, Radi R, Biochim. Biophys. Acta Gen. Subj 2014, 1840, 768–780.

[52]. Ferrer-Sueta G, Campolo N, Trujillo M, Bartesaghi S, Carballal S, Romero N, Alvarez B, Radi R, Chem. Rev 2018, 118, 1338–1408. [PubMed: 29400454]

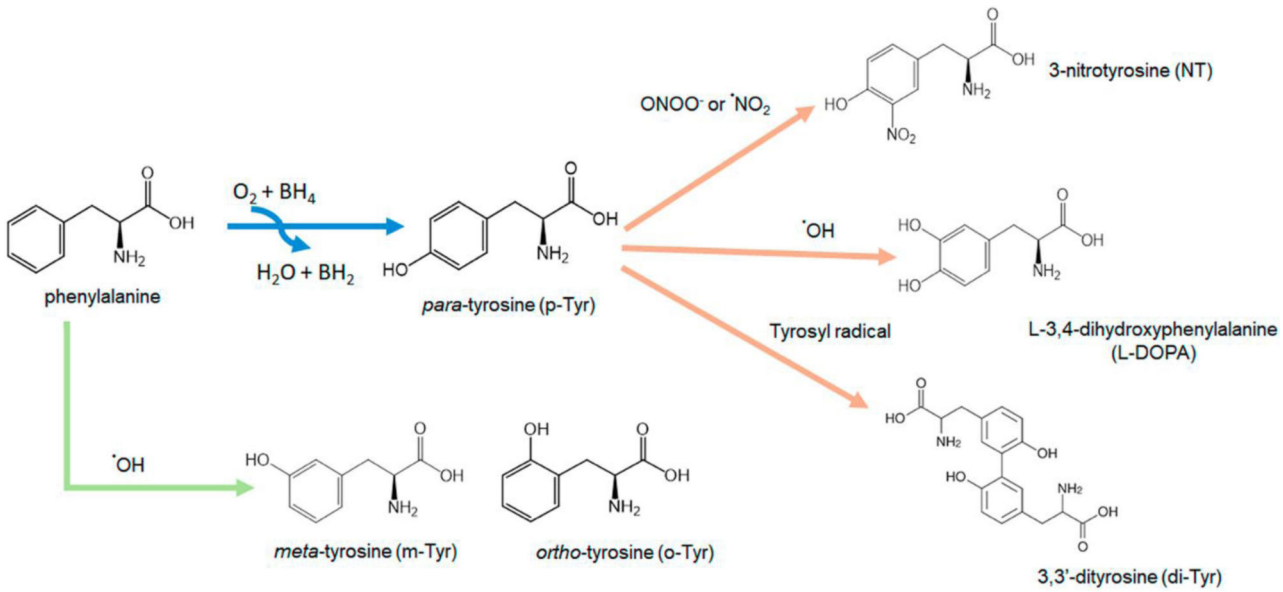

Fig. 1.

Production of modified tyrosine and phenylalanine products due to the reactions of reactive nitrogen and oxygen species with phenylalanine and tyrosine.

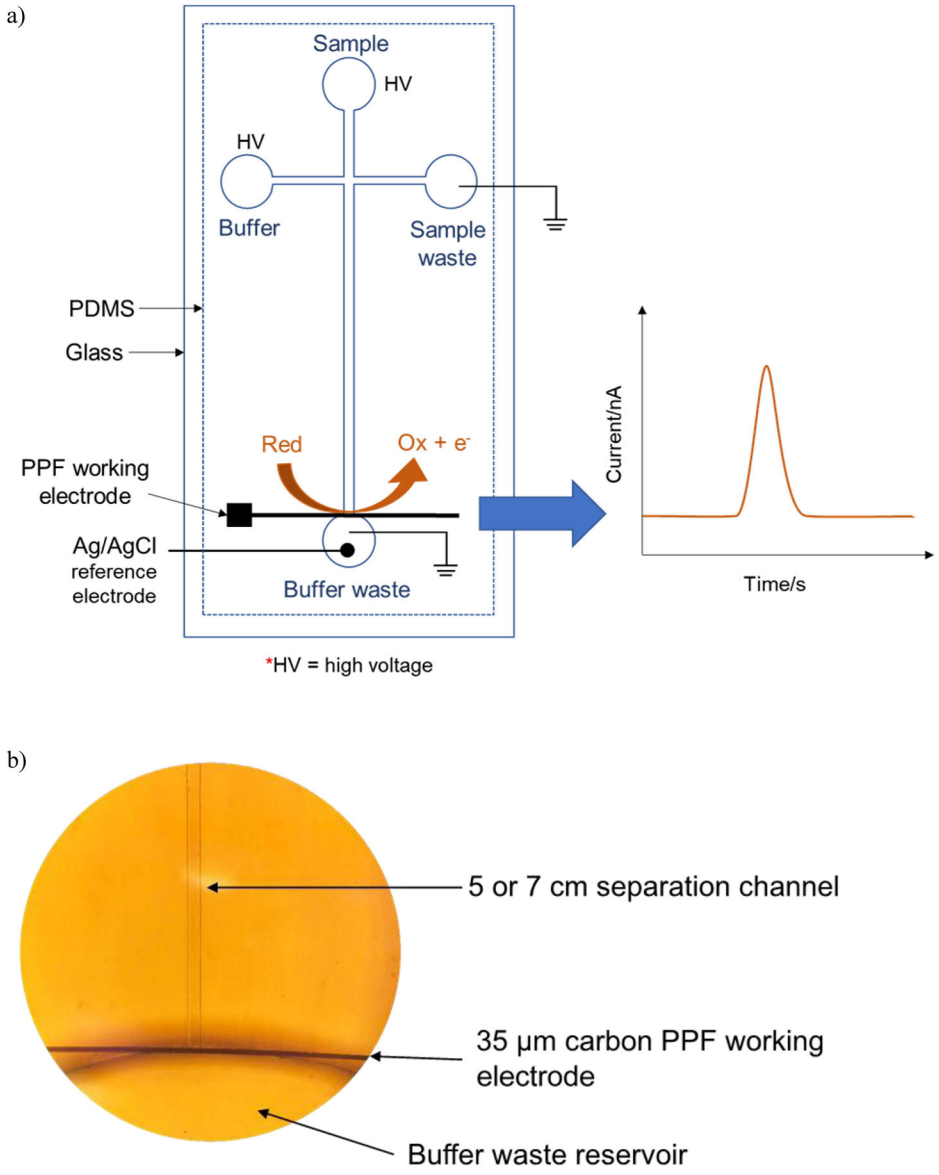

Fig. 2.

a) Diagram of the ME-EC detection system consisting of a PDMS/glass hybrid chip with pyrolyzed photoresist film (PPF) working electrode. b) An image under an inverted microscope (10x magnification) of the 35 μM carbon PPF electrode aligned with the separation channel of the PDMS chip in a pseudo-end channel configuration.

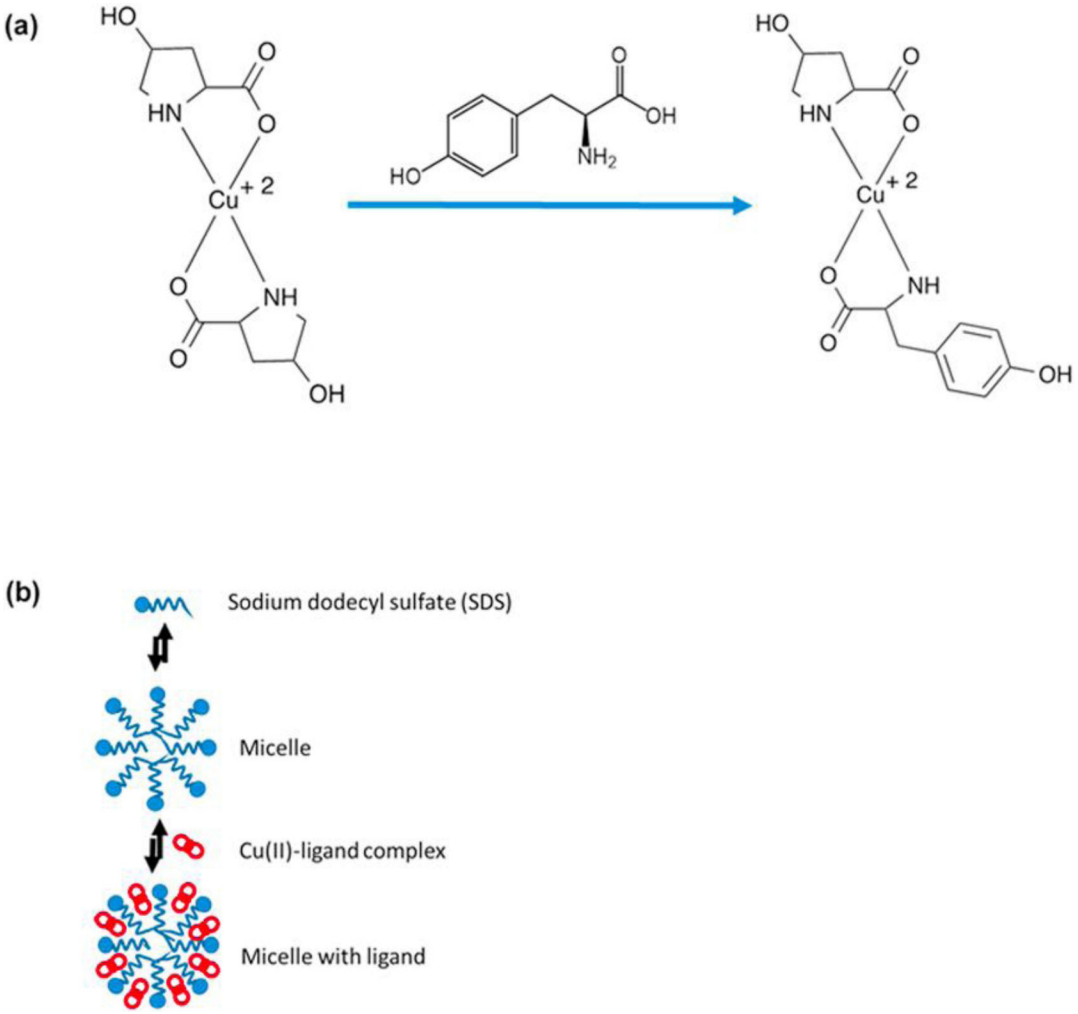

Fig. 3.

Separation mechanism for ligand exchange micellar electrokinetic chromatography (LE-MEKC) (a) 4-hydroxyproline complexes with copper. Tyrosine and its derivatives replace the 4-hydroxyproline leading to a new complex and a change in mobility. (b) Illustration of the partitioning of Cu(II)-ligand complex with micelles, adapted from Chen *et al.* [39].

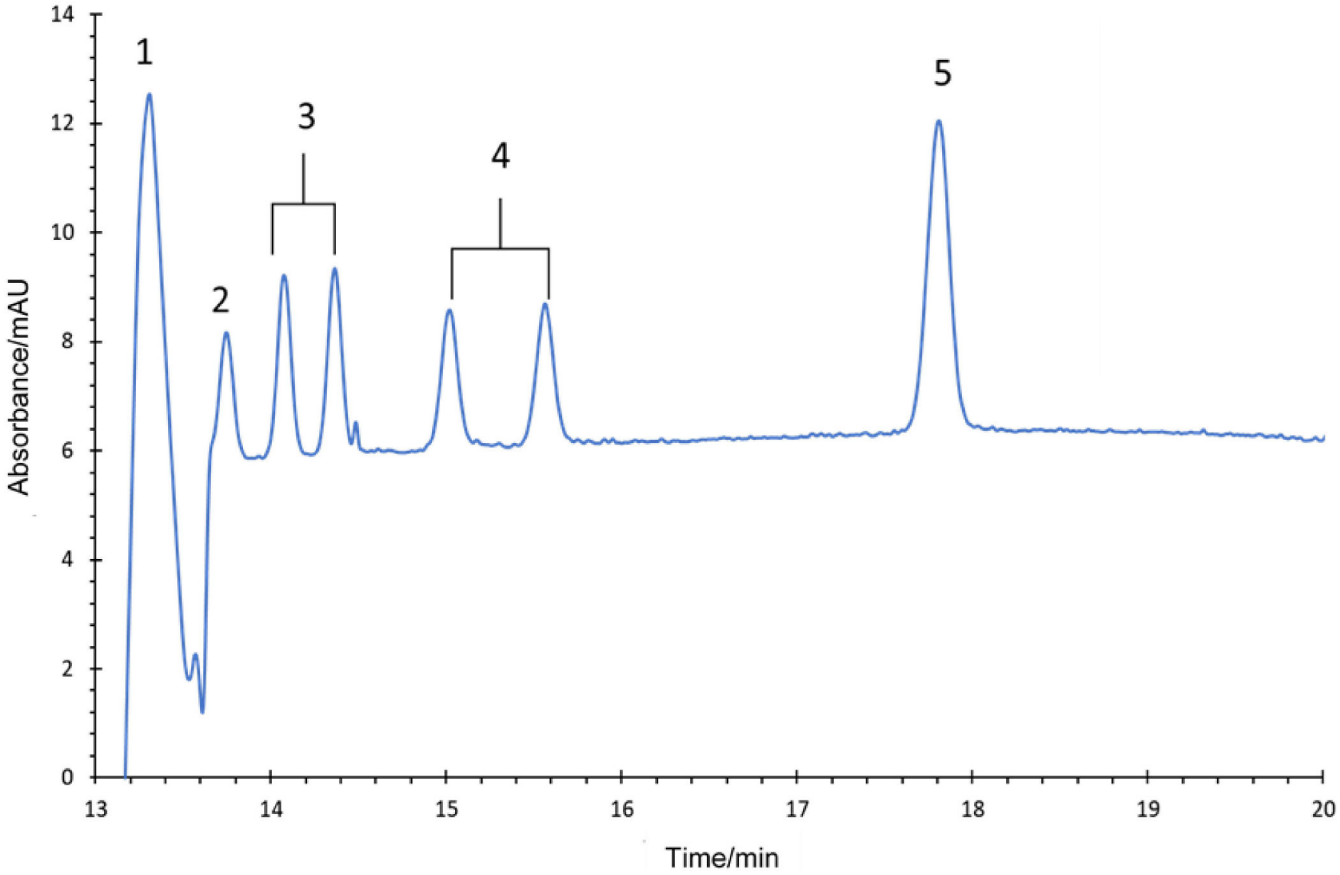

Fig. 4.

Electropherogram of CE-UV detection of L–DOPA, tyrosine isomers and 3-nitrotyrosine standards. The concentrations of each standard were 100 μM. The BGE consisted of 50 mM 4-hydroxyproline and 25 mM Cu(II) at pH 4.5 with 10 mM SDS. A capillary with an effective length of 47.5 cm and a separation voltage of 14 kV were used. UV detection was performed at 208 nm. Peak identities: (1) L–DOPA, (2) p-Tyr (3) DL-m-Tyr, (4) DL-o-Tyr and (5) NT.

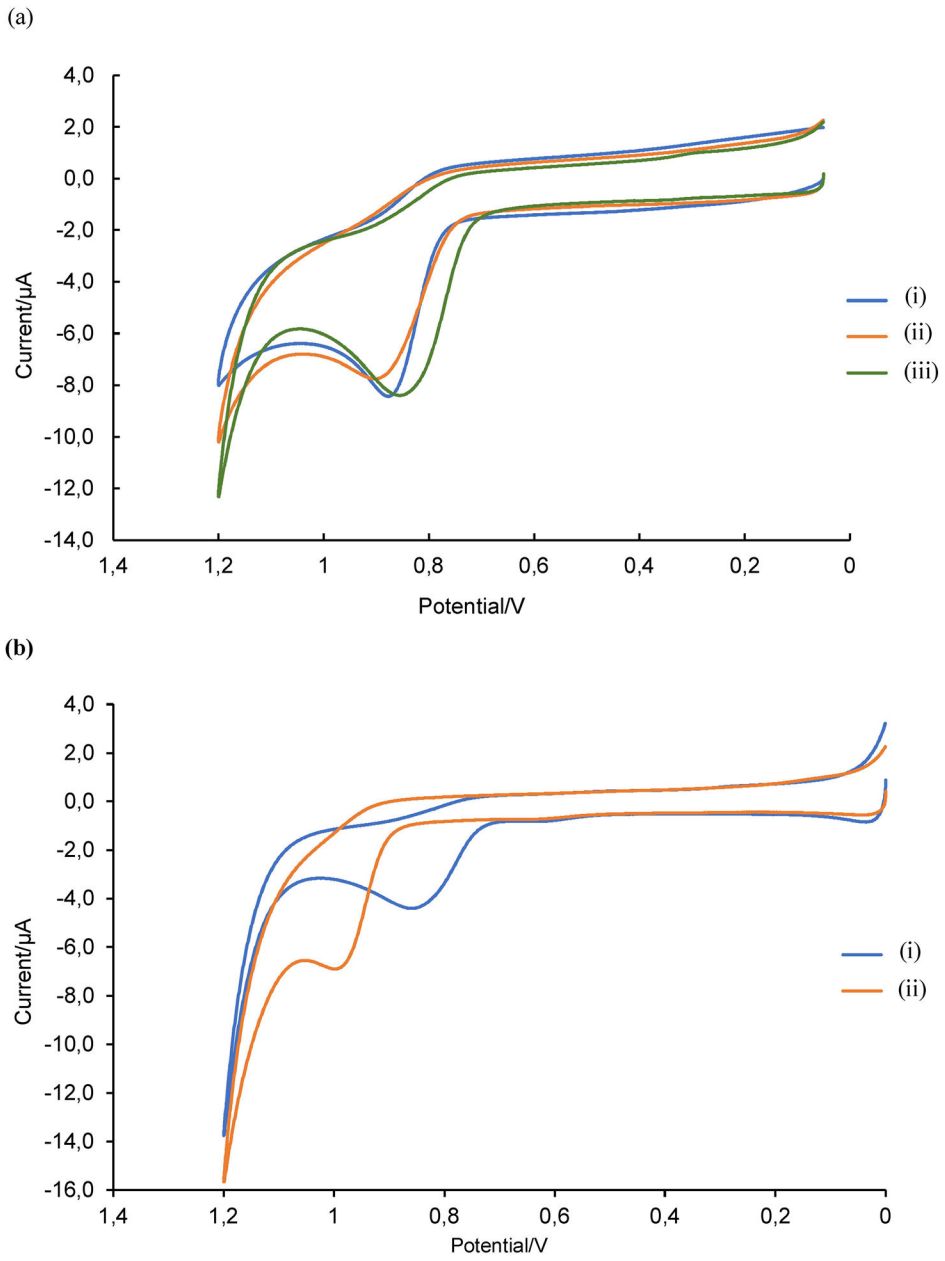

Fig. 5.

a) Cyclic voltammograms of 200 μM p-Tyr dissolved in (i) SE1 = 0.1 M acetate buffer at pH 4.0 (ii) SE2 = 25 mM 4-hydroxyproline and 12.5 mM $CuSO_4$ at pH 4.0 (iii) SE3 = 25 mM 4-hydroxyproline and 12.5 mM $CuSO_4$ at pH 4.0 with 8 mM SDS. A glassy carbon working electrode, Pt auxiliary electrode, and Ag/AgCl reference electrode were used at a scan rate of 100 mV/s. b) Cyclic voltammograms of (i) 200 μM p-Tyr and (ii) 200 μM NT in 25 mM 4-hydroxyproline, 12.5 mM $CuSO_4$ and 15 mm acetate buffer at pH 4.0 with 16.5 mM SDS. A glassy carbon working electrode, Pt auxiliary electrode, and Ag/AgCl reference electrode were used at a scan rate of 100 mV/s.

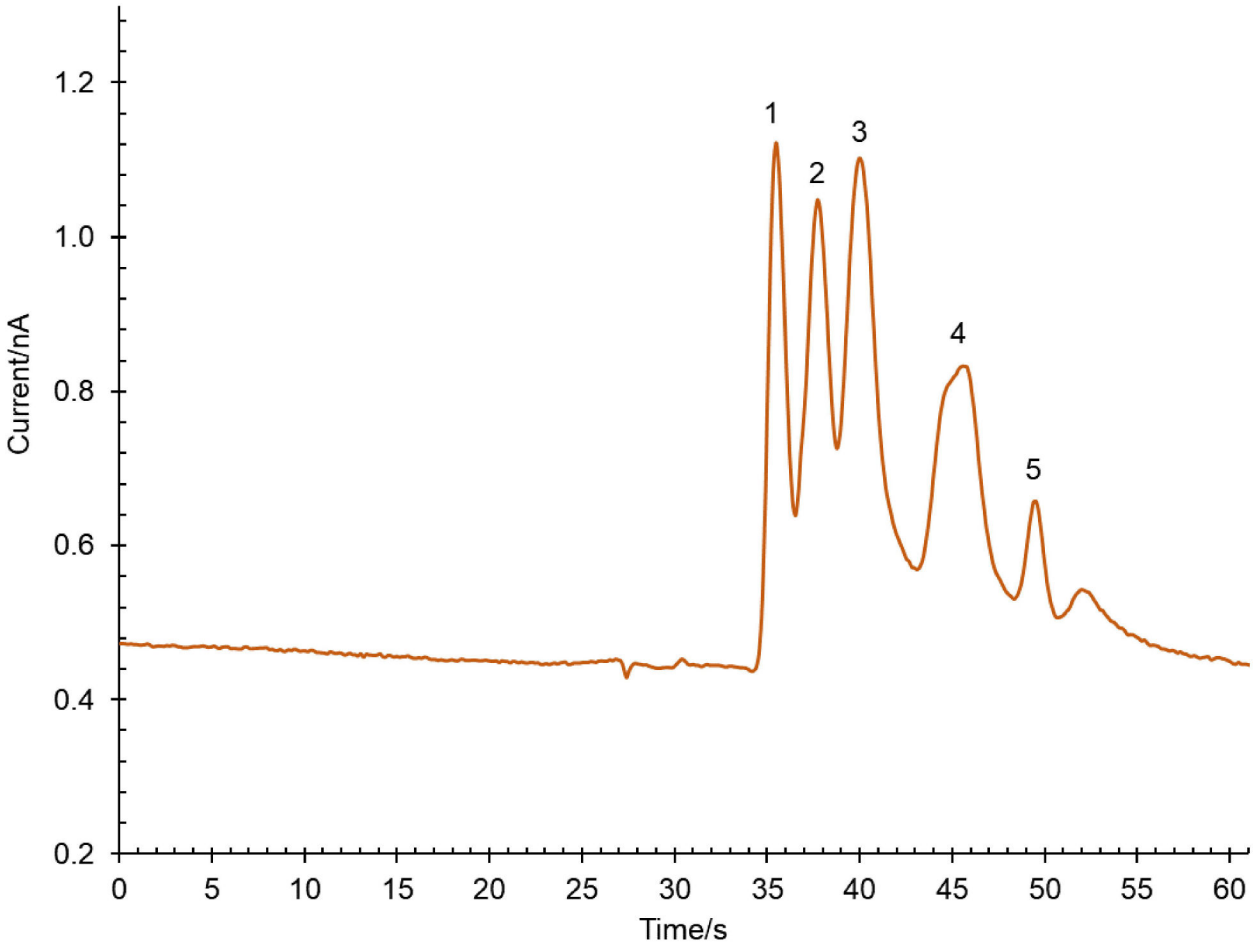

Fig. 6.

ME-EC electropherogram of a mixture of (1) L–DOPA, (2) DL-p-Tyr, (3) DL-m-Tyr, (4) DL-o-Tyr and (5) NT (final concentration = 25 μM for each standard). The BGE consisted of 25 mM 4-hydroxyproline and 12.5 mM Cu(II) at pH 4.5 with 10 mM SDS. A PDMS/glass chip with a 5 cm separation channel and a PPF working electrode were used. Separation voltages: + 1900 V at buffer reservoir and +1600 V at sample reservoir. Applied working electrode (WE) potential was +1.1 V vs. Ag/AgCl.

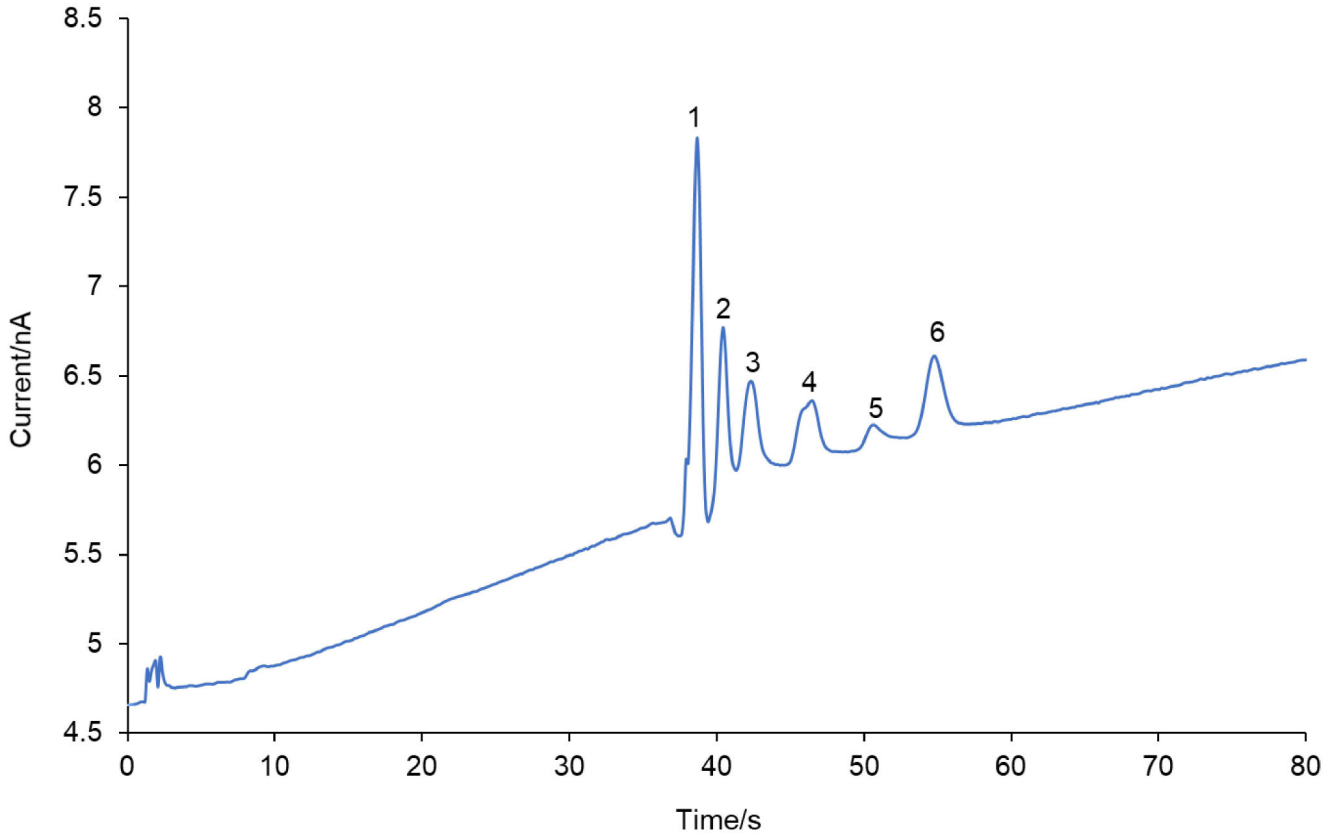

Fig. 7.

Electropherogram for the separation of a mixture containing of all the selected RNOS biomarkers (final concentration = 25 μM for each standard) by ME-EC. The separation buffer consisted of 25 mM 4-hydroxyproline, 12.5 mM Cu(II) and 15 mM ammonium acetate at pH 4.0 with 16.5 mM SDS. A PDMS/glass chip with a 7 cm separation channel was used. Separation voltages: + 2700 V at buffer reservoir & + 2400 V at sample reservoir. Applied WE potential was +1.1 V vs. Ag/AgCl. Peak identities: (1) L–DOPA, (2) L-p-Tyr, (3) DL-m-Tyr, (4) DL-o-Tyr, (5) NT and (6) di-Tyr.

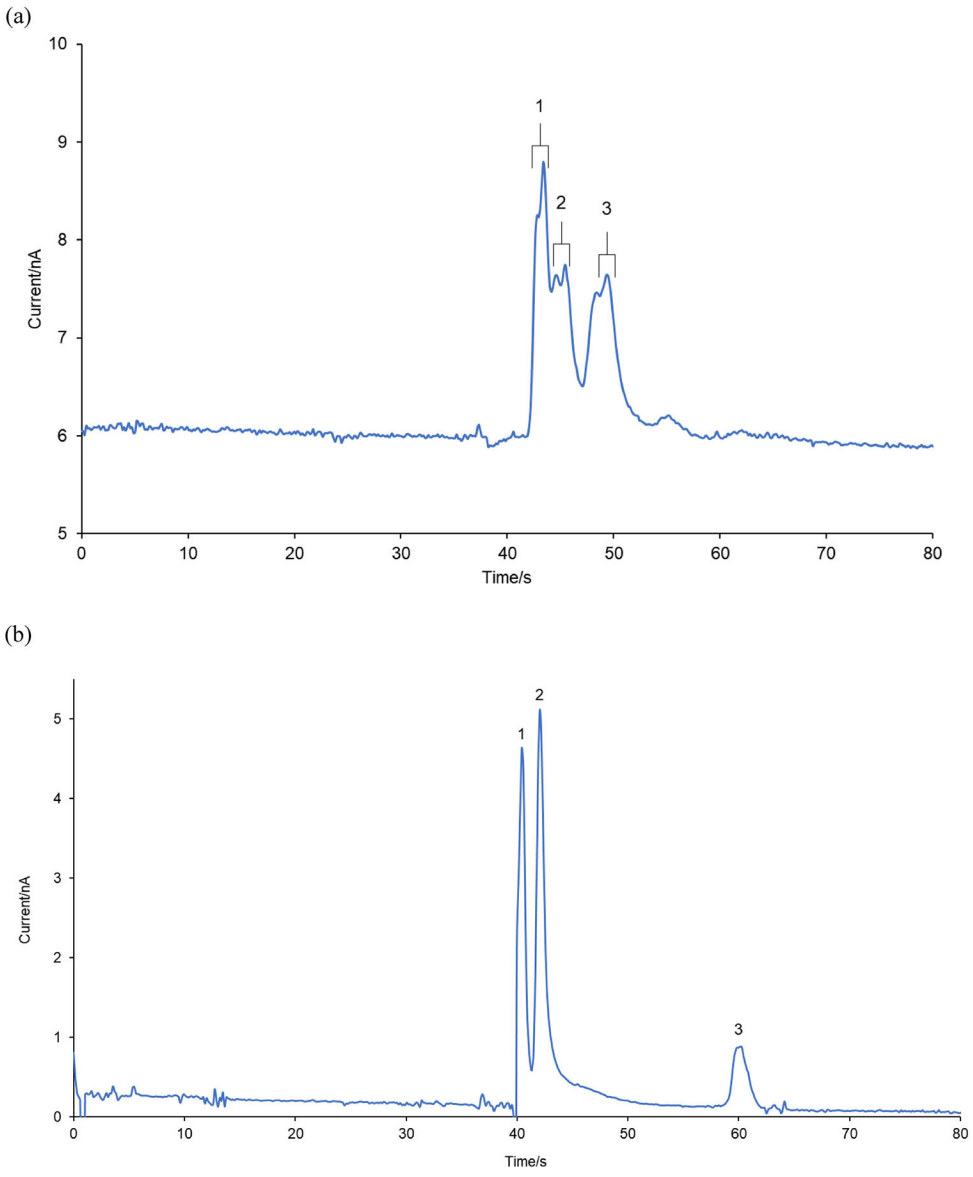

Fig. 8.

Electropherogram for (a) the reaction mixture of the Fenton reaction with 5 mM DL-Phe (Peak identities: (1) DL-p-Tyr (2) DL-m-Tyr and (3) DL-o-Tyr) and (b) the reaction mixture of the Fenton reaction with 1 mM L-p-tyrosine (Peak identities: (1) L–DOPA (2) L-p-Tyr and (3) unknown). Both reaction mixtures were diluted 2-fold with 10 mM acetate buffer at pH 4.0 and injected into microchip with 7 cm separation channel containing 25 mM 4-hydroxyproline, 12.5 mM Cu(II) and 15 mM acetate buffer at pH 4.0 with 16.5 mM SDS. Separation voltages and applied WE potentials were similar to those used in Figure 7.

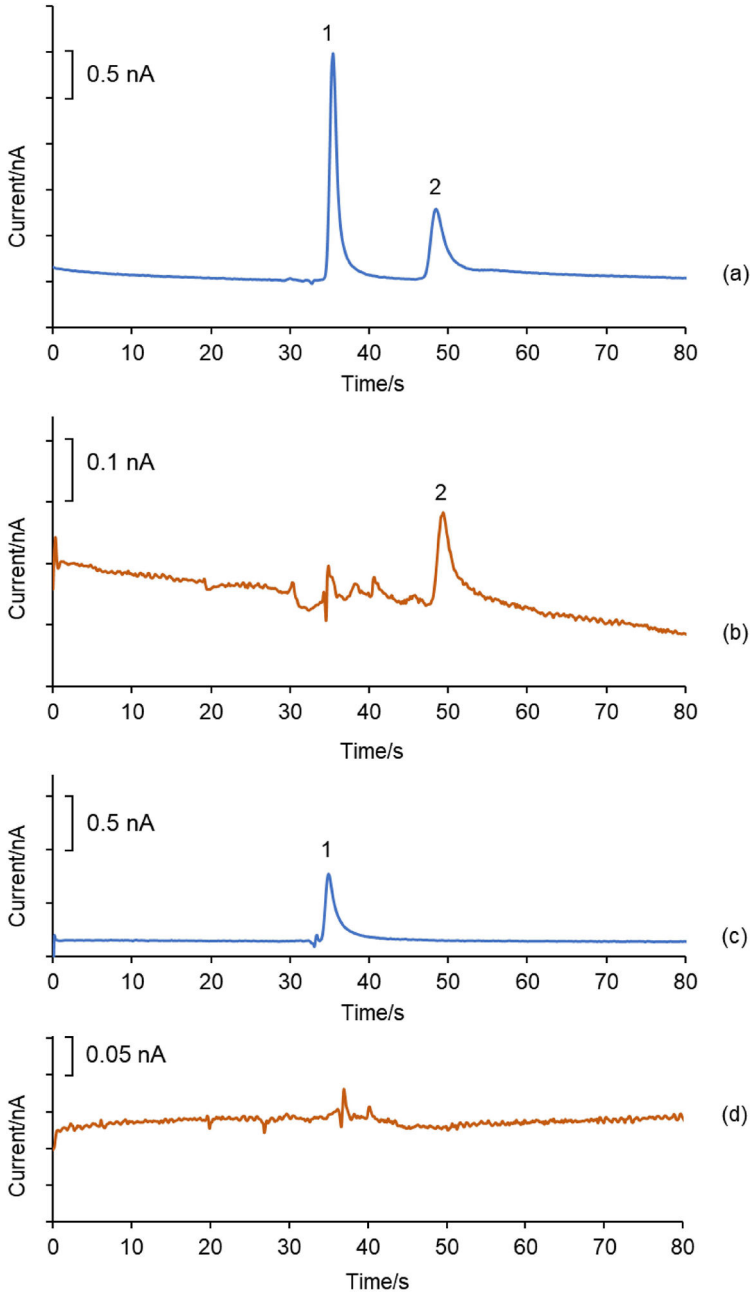

Fig. 9.

Electropherograms of (a) a standard mixture of 50 μM L-p-Tyr and 100 μM NT in BGE (25 mM 4-hydroxyproline, 12.5 mM Cu(II) and 15 mM acetate buffer at pH 4.0 with 16.5 mM SDS) at an applied working electrode potential of +1.1 V vs. Ag/AgCl (b) Sample from the reaction of peroxynitrite with L-p-Tyr (diluted 2-fold with BGE) at an applied working electrode potential of +1.1 V vs. Ag/AgCl, and same standard (c) and reaction mixture (d) at an applied working electrode potential of + 0.9 V vs. Ag/AgCl. Peak identities: (1) L-p-Tyr and (2) NT. Separation voltages were similar to those used in Figure 7.

Table 1.

The effect of background electrolyte composition on the average migration time, standard deviation (SD) and %RSD for the ME-EC analysis of a mixture p-, m-, and o-tyrosine.

BGE composition	Analyte	Average migration time (s)	SD	%RSD
25 mM 4-hydroxyproline, 12.5 mM $CuSO_4$, 16.5 mM SDS at pH 4.0	p-Tyr	59.89	3.00	5.01
	m-Tyr	62.07	2.73	4.39
	o-Tyr	69.96	3.15	4.51
25 mM 4-hydroxyproline, 12.5 mM $CuSO_4$, 16.5 mM SDS, 10 mM ammonium acetate at pH 4.0	p-Tyr	47.44	0.42	0.87
	m-Tyr	50.64	0.48	0.95
	o-Tyr	54.93	0.50	0.91